04,11

Ionic conductivity of cold pressed nanoceramics $Pr_{0.9}Pb_{0.1}F_{2.9}$ obtained by mechanosynthesis of components

© N.I. Sorokin, N.A. Ivanovskaya, I.I. Buchinskaya

Shubnikov Institute of Crystallography „Crystallography and Photonics“, Russian Academy of Sciences, Moscow, Russia

E-mail: nsorokin1@yandex.ru

Received October 13, 2022
Revised October 13, 2022
Accepted October 19, 2022

The impedance spectroscopy in the temperature range 302−779 K was used to study the ionic conductivity of the $Pr_{0.9}Pb_{0.1}F_{2.9}$ nanoceramics, obtained by cold pressing of the powder, mechanically synthesized from components of PbF_2 and PrF_3. The studied material is the solid solution with tysonite-type structure (sp. gr. $P\bar{3}c1$, $Z = 6$) and lattice parameters $a = 7.0906(4)$ and $c = 7.2538(4)$ Å. With increasing temperature, the conductivity of the ceramic increases from $1.9 \cdot 10^{-5}$ to $6.7 \cdot 10^{-2}$ S/cm, and the activation enthalpy of ion transport $\Delta H_\sigma = 0.407 \pm 0.005$ and 0.345 ± 0.005 eV at 302−502 and 502−779 K, respectively. The electrical conductivity mechanism is due to the migration of fluorine vacancies along the boundaries of nanocrystalline grains. The intragranular conductivity of ceramics is close to the electrical conductivity of a single crystal of the same composition. Cold pressed ceramics $Pr_{0.9}Pb_{0.1}F_{2.9}$ can be used as a promising solid electrolyte in „room“ fluorine-ion current sources.

Keywords: ionic conductivity, impedance spectroscopy, fluorides, tysonite structure, cold pressed nanoceramics, mechanosynthesis.

DOI: 10.21883/PSS.2023.01.54982.498

1. Introduction

In condensed systems MF_2-RF_3 (M = Ca, Sr, Ba, Cd, Pb and R = La−Lu, Y) wide regions of crystal phases are formed $R_{1-y}M_yF_{3-y}$ with a tysonite structure (type LaF_3) and a variable number of ions in the unit cell [1–5]. Nonstoichiometric phases $R_{1-y}M_yF_{3-y}$ are anion-deficient heterovalent solid solutions and have high fluorine-ion electrical conductivity [6–10].

The value of the ionic conductivity of the tysonite phase $R_{1-y}M_yF_{3-y}$ of the same chemical composition (R, M, y) strongly depends on the technological form, methods and conditions of synthesis [11]. Fluorine-conducting electrolytes $R_{1-y}M_yF_{3-y}$ are obtained as single crystals (from a melt by directed crystallization methods [12,13]), microceramics with grain size 1−10 μm (solid-phase synthesis with high-temperature annealing, hot pressing [14–16]) and nanoceramics with a grain size of 10−100 nm (mechanosynthesis, mechanical dispersion, co-precipitation from aqueous solutions, solution-melt crystallization [17–20]).

The ionic conductivity of tysonite solid solutions $R_{1-y}M_yF_{3-y}$, M = Ca, Sr, Ba has been studied in detail, while solid solutions with M = Pb, Cd have been investigated to a lesser extent. Synthesis of tysonite phases with PbF_2 is a more complex process than with difluorides of alkaline earth elements (Ca, Sr, Ba). In the work [1,6] provides information on obtaining and studying the radiographic and electrophysical properties of tysonite phases $R_{1-y}Pb_yF_{3-y}$ with R = Pr, Nd obtained by the directional crystallization from the melt. The growth of crystals $Pr_{1-y}Pb_yF_{3-y}$ ($0 \le y \le 0.09$) from the melt is hampered by a large difference in the melting temperatures of PrF_3 (1677 K) and PbF_2 (1099 K) and high volatility of lead difluoride.

Recently, studies of the ionic conductivity of tysonite phases $R_{1-y}M_yF_{3-y}$ in nanocrystalline form have attracted close attention. Nanoceramic materials $R_{1-y}M_yF_{3-y}$ (especially $La_{1-y}Ba_yF_{3-y}$) are widely used in fluorine-ion sources new generation current [21–24]. The results obtained showed that nanoceramics $R_{1-y}M_yF_{3-y}$ [18,19,21–27] have rather low values of „room“ ionic conductivity ($10^{-8}-10^{-6}$ S/cm) and require high-temperature annealing to increase it. A significant factor affecting the anionic conductivity of nanoceramic samples $R_{1-y}M_yF_{3-y}$ is the migration of fluorine vacancies at the boundaries of nanocrystalline grains [28–30].

The possibility of obtaining nanoscale particles $La_{0.85}Pb_{0.15}F_{2.85}$ by mechanosynthesis is shown in [31]. There is no information in the scientific literature about the purposeful production and study of other lead-containing tysonite nanoceramics.

The aim of the work is the preparation by mechanosynthesis followed by cold pressing of a nanoceramic solid electrolyte $Pr_{1-y}Pb_yF_{3-y}$ and measurement of its ionic conductivity.

2. Experiment

Commercial reagents PbF_2 (purity 99.995% Sigma-Aldrich) and PrF_3 (purity 99.99% Lanhit) were used as

initial components. For purification from oxygen-containing impurities, powdered reagents were previously dried in vacuum and melted in an atmosphere $He + CF_4$.

For mechanical grinding, a high-energy planetary ball mill Retsch PM-200 was used (the volume of the grinding cup is 50 cm^3, 13 steel balls with a diameter of 10 mm, the ratio of the mass of the balls to the mass of the substance 17 : 1), inert atmosphere Ar (99.9995%). The rotation speed was 600 rpm, the grinding energy intensity ~ 0.2 W/g.

Mechanical melting of a solid solution $Pr_{1-y}Pb_yF_{3-y}$ from a mixture of components $PrF_3 : PbF_2$ in the ratio 9 : 1 was conducted during 12 h. Details of the technique of obtaining fluoride solid solutions by mechanosynthesis are described in [27,32,33].

Cold pressed ceramics $Pr_{1-y}Pb_yF_{3-y}$ are prepared at room temperature on a Carl Zeiss manual press. Pressing was carried out at a static pressure of 600 MPa for 10 min. Weighing cylindrical samples and calculating their volume from geometric dimensions showed that the density of cold-pressed ceramics is 80−85% of the X-ray density of the solid solution $Pr_{0.9}Pb_{0.1}F_{2.9}$ [1]. In [34] it is indicated that the agglomeration of nanoparticles in a powder sample leads to a low density of cold-pressed ceramics of tysonite $La_{0.95}Ba_{0.05}F_{2.95}$.

Registration of diffraction patterns of mechanosynthesis products was carried out using a powder X-ray diffractometer Rigaku MiniFlex-600 in the angle range $2\theta = 10-100°$, radiation CuK_α (40 kV, 15 mA, NiK_β-filter). X-ray diffration (XRD) analysis for the search and identification of crystal phases present in the samples was performed in the PXDRL (Rigaku) program using the ICDD PDF-2 database (2017). The calculation of the parameters of the elementary cells of the tysonite phase within the framework of sp. gr. $P\bar{3}c1$ was carried out by the method of full-profile analysis of Le Bail using the software Jana-2006.

The sample for electrophysical measurements was a cylinder with a thickness of 1.65 mm and a diameter of 3 mm. Inert electrodes (silver paste Leitsilber) were applied to the end surfaces of the sample. Static dc-electrical conductivity σ_{cer} of the ceramic sample was measured by impedance spectroscopy in the temperature range 302−779 K in the cooling mode. Temperature measurements $\sigma_{cer}(T)$ were carried out on stabilized (stabilization time 15−30 min) points in increments of ~ 25 K. Impedance measurements $Z^*(\omega)$ electrochemical cells Ag — ceramics — Ag were performed in the frequency ranges $5-5 \cdot 10^5$ Hz and resistances $1-10^7\ \Omega$ (Tesla Impedance meter BM−507), in vacuum ~ 1 Pa. For comparison, impedance measurements of cold-pressed ceramics of the tysonite component PrF_3 were also carried out. The description of the experimental setup and the method of electrophysical measurements are given in [35]. Relative measurement error $Z^*(\omega)$ was 5%.

Impedance measurements allow us to reliably determine the bulk resistance R_b of ceramics by the intersection of the impedance hodographs $Z^*(\omega)$ for electrochemical cells with an active resistance axis. The values of dc-conductivities were determined by the formula

$$\sigma_{cer} = h/SR_b, \tag{1}$$

where h is the thickness of the sample and S is the area of the electrode.

The presence in the impedance spectra of the blocking effect from inert (silver) electrodes at low frequencies indicates the ionic nature of the electrical transfer in the studied ceramics. The ion transport in a solid solution of $Pr_{1-y}Pb_yF_{3-y}$ of highly charged (Pb^{2+}, Pr^{3+}) cations is unlikely, therefore ionic conductivity is due to ions F^-. This is directly indicated by the results of the F^{19} NMR study of tysonite crystals $R_{1-y}M_yF_{3-y}$ (R = La, Ce, Nd; M = Ca, Sr, Ba, Cd) [19,36–38], in which high ion diffusion was detected F^-.

3. Discussion of results

According to the XRD results, the lattice parameters of the initial components are $a = 5.939(4)$ Å for PbF_2 (type of fluorite, sp. gr. $Fm\bar{3}m$) and $a = 7.0769(4)$, $c = 7.2378(5)$ Å for PrF_3 (type of tysonite, sp. gr. $P\bar{3}c1$). Mechanosynthesis was carried out in two modes, duration $\tau = 1$ and 12 h with composition control. Fig. 1 shows diffractograms of the initial components (*1*) and (*2*) and the products of mechanosynthesis with a duration of $\tau = 1$ h (*3*) and 12 h (*4*). The XRD analysis showed that during 1 h the synthesis has completely passed, one tysonite phase $Pr_{1-y}Pb_yF_{3-y}$ is fixed with the parameters of the unit cell $a = 7.0948(3)$ and $c = 7.2522(3)$ Å. Admixture of the initial components within the accuracy of the method is not observed.

The average size of the coherent scattering regions (**OCD**) of X-rays was estimated from the width of diffraction reflexes, which, in the first approximation, corresponds to the average size of crystalline particles. Calculations were carried out according to the formula of Selyakov–Scherrer [33]:

$$B_s = K\lambda/\beta\cos\theta, \tag{2}$$

where K — coefficient for grain shape accounting ($K \approx 0.94$ for spherical particles), λ — radiation wavelength (in our case $\lambda_{CuK\alpha} = 0.154$ nm), θ — the Bragg angle for the diffraction peak, β — the observed width of the diffraction peak at half the height (in radians). The instrumental component of the broadening was neglected in the evaluation. The resulting OCD size is 13 ± 3 nm.

As a result of continued grinding to $\tau = 12$ h lattice parameters change slightly: $a = 7.0906(4)$ and $c = 7.2538(4)$ Å, diffraction lines widen, reflexes (022) and (121) responsible for belonging to sp. gr. $P\bar{3}c1$, practically merge with the background. Estimation of the size of OCD by the formula (2) gives a value of 7 ± 3 nm.

Thus, the duration of mechanical synthesis $\tau = 1$ h is quite sufficient to obtain a solid solution of $Pr_{0.9}Pb_{0.1}F_{2.9}$ with lattice parameters close to the parameters of a saturated

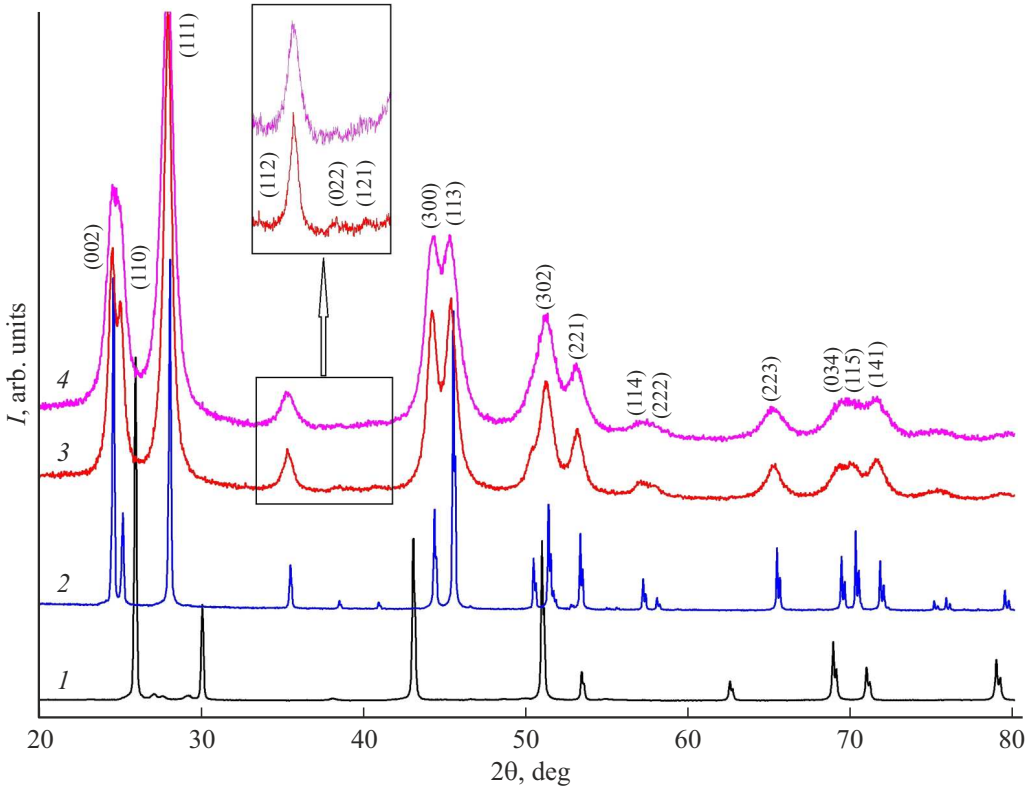

Figure 1. Diffractograms of initial components and solid solution: *1* — PbF_2 (sp. gr.$Fm\bar{3}m$), *2* — PrF_3 (sp. gr. $P\bar{3}c1$), *3* and *4* — $Pr_{0.9}Pb_{0.1}F_{2.9}$ (sp. gr. $P\bar{3}c1$), obtained by mechanosynthesis with a duration of $\tau = 1$ and 12 h, respectively.

solid solution according to [1], where the solubility limit of PbF_2 in PrF_3 is defined as 9 ± 2 mol.%.

The sample for electrophysical measurements was compressed from a nanopowder obtained by mechanosynthesis with a duration of $\tau = 12$ h with a smaller value of OCD. Figure 2 shows the impedance hodograph $Z^*(\omega)$ electrochemical cell with ceramics $Pr_{0.9}Pb_{0.1}F_{2.9}$ cold pressing and Ag electrodes at 302 K. It is possible to separate the contributions to the total resistance R_b from the resistance of the grain volume R_{ig} and the resistance of the grain contacts R_{gb}. Here $R_{cer} = R_{ig} + R_{gb}$ is total resistance of the ceramic sample, R_{ig} is intragrain (interior grain) resistance, R_{gb} is intergrain (grain boundary) resistance. The conductivity values of σ_{cer}, σ_{ig} and σ_{gb} are $1.9 \cdot 10^{-5}$, $2.3 \cdot 10^{-4}$ and $2.0 \cdot 10^{-5}$ S/cm, respectively. The intragrain conductivity of σ_{ig} nanoceramics $Pr_{0.9}Pb_{0.1}F_{2.9}$ does not differ much from the electrical conductivity ($4.5 \cdot 10^{-4}$ S/cm [39,40]) of a single crystal $Pr_{0.9}Sr_{0.1}F_{2.9}$. It can be seen that the main contribution to the ionic conductivity of the sample is made by the intergranular resistance of R_{gb} nanoceramics.

Fig. 3 shows the temperature dependence of the ionic conductivity of cold-pressed ceramics $Pr_{0.9}Pb_{0.1}F_{2.9}$ in the temperature range 302–779 K in cooling mode. The increase in the electrical conductivity from 302 to 779 K is $3.5 \cdot 10^3$ times. The conductometric data was processed

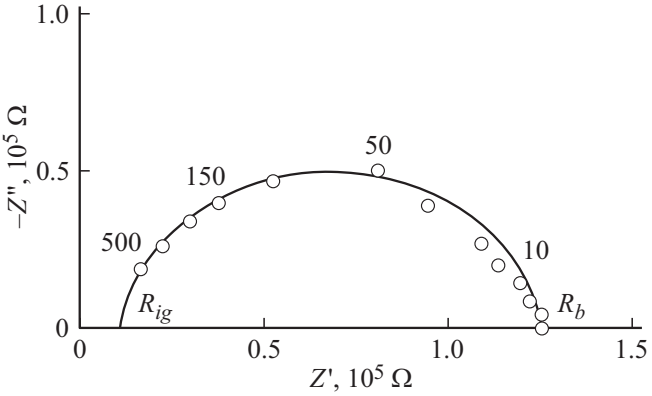

Figure 2. Impedance hodograph $Z^*(\omega)$ for the system Ag — ceramics — Ag at 302 K. Nanocrystalline powder $Pr_{0.9}Pb_{0.1}F_{2.9}$ prepared by mechanical synthesis ($R_b = 1.25 \cdot 10^5\ \Omega$, $R_{ig} = 1 \cdot 10^4\ \Omega$). The numbers at the dots indicate the frequency in kHz.

in compliance with the Arrhenius–Frenkel equation

$$\sigma_{cer} T = \sigma_0 \exp(-\Delta H_\sigma / kT), \qquad (3)$$

where σ_0 is the pre-exponential factor of electrical conductivity and ΔH_σ is the enthalpy of ion transfer activation. On the dependency $\sigma_{cer}(T)$ $Pr_{0.9}Pb_{0.1}F_{2.9}$ a bend is observed at 502 K, which is a characteristic feature for tysonite

Table 1. Crystal lattice parameters (a, c), the average size of crystal grains (B_s) and the parameters of the Arrhenius–Frenkel equation for nanoceramics $Pr_{0.9}Pb_{0.1}F_{2.9}$, PrF_3 and $La_{0.9}Ba_{0.1}F_{2.9}$

Composition	a, c, B_s, nm	σ_0, SK/cm	ΔH_σ	σ_{cer}, S/cm
$Pr_{0.9}Pb_{0.1}F_{2.9}$	$a = 0.70906$ $c = 0.72538$ $B_s = 7$	$8.99 \cdot 10^3$ $3.67 \cdot 10^4$	0.345 (502–779 K) 0.407 (302–502 K)	$6.0 \cdot 10^{-3}$ (500 K)
PrF_3	$a = 0.70769$ $c = 0.72378$	$1.76 \cdot 10^2$	0.396 (551–798 K)	$3.6 \cdot 10^{-5}$ (500 K)
$La_{0.9}Ba_{0.1}F_{2.9}$ [18]	$a = 0.722$ $c = 0.739$ $B_s = 13$	$3.54 \cdot 10^5$	0.55 (293–473 K)	$1.0 \cdot 10^{-3}$ (473 K)
$La_{0.9}Ba_{0.1}F_{2.9}$ [26]	$B_s = 10$–20	–	0.54 (293–473 K)	$2.4 \cdot 10^{-4}$ (473 K)

fluorides. Parameters of the Frenkel–Arrhenius equation for nanoceramics $Pr_{0.9}Pb_{0.1}F_{2.9}$, PrF_3 (real work) and $La_{0.9}Ba_{0.1}F_{2.9}$ (literature data) are given in Table 1.

The value σ_{cer} at 773 K for nanoceramics $Pr_{0.9}Pb_{0.1}F_{2.9}$ in comparison with PrF_3 exceeds by a factor of 110. The obtained values of the enthalpy of activation of ionic conductivity for ceramics $Pr_{0.9}Pb_{0.1}F_{2.9}$ and PrF_3 correspond to the migration energies of fluorine vacancies in tysonite structures $R_{1-y}M_yF_{3-y}$ [14,15,39–41].

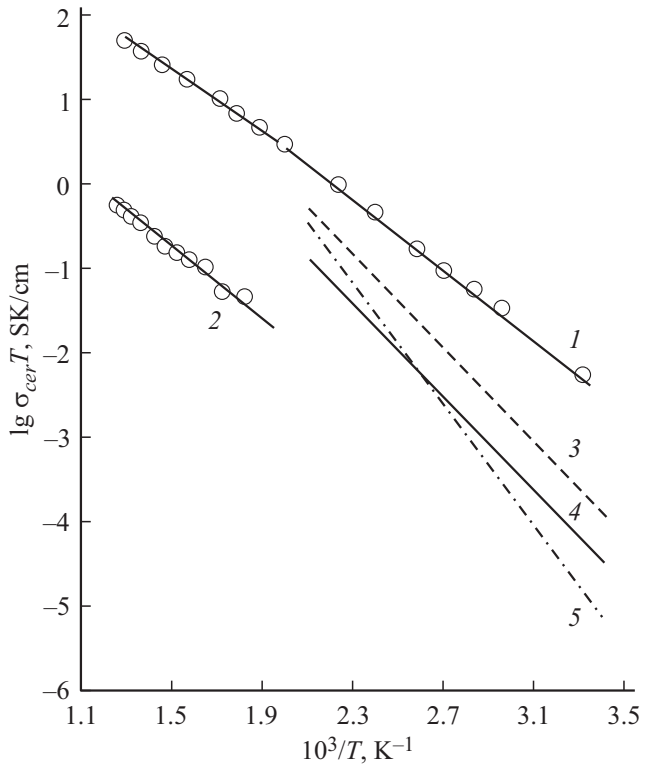

Figure 3. Temperature dependence of ionic conductivity $\sigma_{cer}(T)$ of nanoceramic samples: *1* — $Pr_{0.9}Pb_{0.1}F_{2.9}$, *2* — PrF_3, *3* — $La_{0.9}Ba_{0.1}F_{2.9}$ [18], *4* — $La_{0.9}Ba_{0.1}F_{2.9}$ [26], *5* — $La_{0.8}Sn_{0.2}F_{2.8}$ [43].

Table 2. Composition, method of preparation and ionic conductivity of tysonite ceramics with cold pressing of reaction products in systems RF_3–MF_2 (R = Pr, La; M = Pb, Sn, Sr, Ba) and fluorite ceramics in the PbF_2–CdF_2

Solid solution	Method synthesis	T, K	σ_{cer}, S/cm	Reference
$Pr_{0.9}Pb_{0.1}F_{2.9}$	MS	302	$1.9 \cdot 10^{-5}$	Real study
$Pr_{0.958}Pb_{0.042}F_{2.958}$ $Pr_{0.882}Pb_{0.118}F_{2.882}$	DC	296	$7.3 \cdot 10^{-5}$ $3.1 \cdot 10^{-5}$	[6]
$Pr_{0.95}Sr_{0.05}F_{2.95}$	MD	293	$5 \cdot 10^{-7}$	[42]
$La_{0.85}Pb_{0.15}F_{2.85}$	MS	298	$2.4 \cdot 10^{-6}$	[31]
$La_{0.8}Sn_{0.2}F_{2.8}$	MS	293	$3.2 \cdot 10^{-8}$	[43]
$La_{0.8}Ca_{0.2}F_{2.8}$	MS	298	$1 \cdot 10^{-6}$	[27]
$La_{0.95}Sr_{0.05}F_{2.95}$	MD	293	$5 \cdot 10^{-6}$	[17]
$La_{0.95}Ba_{0.05}F_{2.95}$	MS	293	$2 \cdot 10^{-7}$	[18]
$La_{0.9}Ba_{0.1}F_{2.9}$	MS	293 293 350	$1 \cdot 10^{-7}$ $4.2 \cdot 10^{-7}$ $7 \cdot 10^{-7}$	[26] [18] [19]
$Pb_{0.67}Cd_{0.33}F_2$	MS MD	297 297	$2.4 \cdot 10^{-5}$ $5.1 \cdot 10^{-5}$	[32]

Note. MS — mechanical synthesis, MD — mechanical dispersion, DC — directional crystallization.

Table 2 compares the ionic conductivity of tysonite ceramics obtained by cold pressing of reaction products in the systems RF_3–MF_2 (R = Pr, La; M = Pb, Sn, Sr, Ba) and PbF_2–CdF_2. It can be seen that the high conductometric characteristics of cold-pressed ceramics are $Pr_{0.9}Pb_{0.1}F_{2.9}$ allow us to consider it as a promising fluoroconducting solid electrolyte with a tysonite structure for use in fluorine-ion current sources.

4. Conclusion

Using the example of a highly conductive ceramic electrolyte $Pr_{1-y}Pb_yF_{3-y}$, a promising technique for producing lead-containing tysonite solid electrolytes is proposed, which uses a solid solution in the form of a nanopowder obtained by mechanosynthesis of PrF_3 and PbF_2 components. The product of mechanosynthesis is a solid solution of $Pr_{0.9}Pb_{0.1}F_{2.9}$ with a tysonite structure. To complete the process of mechanosynthesis, the grinding duration $\tau = 1$ h is sufficient.

The ionic conductivity of cold-pressed ceramics was measured $Pr_{0.9}Pb_{0.1}F_{2.9}$ in the temperature range 302−779 K. „Room" ionic conductivity is $1.9 \cdot 10^{-5}$ S/cm at 302 K. High conductometric characteristics of cold pressed ceramics $Pr_{0.9}Pb_{0.1}F_{2.9}$ allow us to consider it as a promising fluorine-ion coductive solid electrolyte with a tysonite structure for low-temperature studies.

Acknowledgments

The authors thank D.N. Karimov and A.G. Ivanov for discussing the work.

Funding

The work was carried out with the support of the Ministry of Science and Higher Education as part of the work on the State assignment using the equipment of the Center for Collective Use of the Federal Scientific Research Center „Crystallography and Photonics" RAS.

Conflict of interest

The authors declare that they have no conflict of interest.

References

[1] I.I. Buchinskaya, N.A. Arkharova, A.G. Ivanova, D.N. Karimov. Kristallografiya **65**, 147 (2020). (in Russian).
[2] B.P. Sobolev, N.I. Tkachenko. J. Less-Common. Met. **85**, 155 (1982).
[3] B.P. Sobolev, K.B. Seiranian. J. Solid State Chem. **39**, 337 (1981).
[4] B.P. Sobolev, P.P. Fedorov. J. Less-Common. Met. **60**, 33 (1978).
[5] M. El Omari, J.M. Reau, J. Senegas. Phys. Status Solidi A **121**, 415 (1990).
[6] N.I. Sorokin, D.N. Karimov, I.I. Buchinskaya. Elektrokhimiya **57**, 465 (2021). (in Russian).
[7] B.P. Sobolev, N.I. Sorokin, N.B. Bolotina. Photonic & electronic properties of fluoride materials / Eds A. Tressaud, K. Poeppelmeier. Elsevier, Amsterdam (2016) P. 465.
[8] N.I. Sorokin, B.P. Sobolev, E.A. Krivandina, Z.I. Zhmurova. Kristallografiya **60**, 123 (2015). (in Russian).
[9] B.P. Sobolev, N.I. Sorokin, E.A. Krivandina, Z.I. Zhmurova. Kristallografiya **59**, 609 (2014). (in Russian).
[10] M. El Omari, J. Senegas, J.M. Reau. Solid State Ionics **107**, 281 (1998).
[11] N.I. Sorokin, B.P. Sobolev. Kristallografiya **61**, 468 (2016). (in Russian).
[12] I.I. Buchinskaya, D.N. Karimov. Crystals **11**, 629 (2021). https://doi.org/10.3390/cryst11060629
[13] V. Vasyliev, P. Molina, M. Nakamura, E.G. Villora, K. Shimamura. Opt. Mater. **33**, 1710 (2011).
[14] T. Takahashi, H. Iwahara, T. Ishikava. J. Electrochem. Soc. **124**, 280 (1977).
[15] I.V. Murin, O.V. Glumov, Yu.V. Amelin. ZhPKh **53**, 1474 (1980). (in Russian).
[16] N.I. Sorokin, A.N. Smirnov, P.P. Fedorov, B.P. Sobolev. Elektrokhimiya **45**, 641 (2009). (in Russian).
[17] N.I. Sorokin, N.A. Ivanovskaya, B.P. Sobolev. Kristallografiya **59**, 286 (2014).(in Russian).
[18] C. Rongeat, M. Anji Reddy, R. Witter, M. Fichtner. ACS Appl. Mater. Interfaced. **6**, 2103 (2014).
[19] A. Duvel, J. Bednarcik, V. Sepelak, P. Heitjans. J. Phys. Chem. C **118**, 7117 (2014).
[20] P.P. Fedorov, A.A. Luginina, S.V. Kuznetsov, V.V. Osiko. J. Fluorine Chem. **132**, 1012 (2011).
[21] M. Anji Reddy, M. Fichtner. J. Mater. Chem. **21**, 17059 (2011).
[22] I. Mahammad, R. Witter, M. Fichtner, M. Anji Reddy. ASC Appl. Energy Mater. **2**, 1553 (2019).
[23] K. Motohashi, T. Nakamura, Y. Kimura, Y. Uchimoto, K. Amezava. Solid State Ionics. **338**, 113 (2019).
[24] L. Liu, L. Yang, D. Shao, K. Luo, C. Zou, Z. Luo, X. Wang. Ceram. Int. **46**, 20521 (2020). doi.org/10.1016/j.ceramint.2020.05.161
[25] M. Anji Reddy, M. Fichtner. J. Phys. Chem. C **21**, 17059 (2011).
[26] M. Gombotz, V. Pregartner, I. Hanzu, H. Martin, R. Wilkening. Nanomaterials **9**, 1517 (2019). https://doi.org/10.3390/nano9111517
[27] B.P. Sobolev, I.A. Sviridov, V.I. Fadeeva, S.N. Sulyanov, N.I. Sorokin, Z.I. Zhmurova, I.I. Khodos, A.S. Avilov, M.A. Zaporozhets. Kristallografiya **53**, 919 (2008). (in Russian).
[28] L.N. Patro. J. Solid State Electrochem. **24**, 2219 (2020). https://doi.org/10.1007/s10008-020-04769-x
[29] A.K. Ivanov-Shits, L.N. Demyanets. Kristallografiya **48**, S170 (2003). (in Russian).
[30] K.R. Achary, Y. Braskara, L.N. Patro. Mater. Lett. **301**, 130337 (2021).
[31] Ts. Tzi, I.O. Trefilov. Mater. international. youth. sci. forum „Lomonosov-2021" / Ed. I.A. Aleshkovsky, A.V. Andriyanov, E.A. Antipov, E.I. Zimakova. [electronic resource]. M.: MAKS Press (2021).
[32] N.I. Sorokin, I.I. Buchinskaya, N.A. Ivanovskaya, A.S. Orekhov. Kristallografiya **67**, 318 (2022). (in Russian).
[33] V.V. Boldyrev. Eksperimental'nye metody v mekhanokhimii tverdykh neorganicheskikh veshchestv (Experimental methods in mechanochemistry of solid inorganic substances). Nauka, Novosibirsk (1983). 65 p. (in Russian).
[34] J. Chable, A.G. Martin, A. Bourdin, M. Body, C. Legein, A. Jouauneaux, M.P. Crosnier-Lopez, C. Galven, B. Dieudonne, M. Leblanc, A. Demourgues, V. Maisonneuve. J. Alloys Comp. **692**, 980 (2017). https://doi.org/10.1016/j.jallcom.2016.09.135
[35] A.K. Ivanov-Shitz, N.I. Sorokin, P.P. Fedorov, B.P. Sobolev. FTT **25**, 1748 (1983). (in Russian).
[36] F. Fujara, D. Kruk, O. Lips, A.F. Privalov, V. Sinitsyn, S. Stork. Solid State Ionics **179**, 2350 (2008).

[37] M. El Omari, J. Senegas, J.M. Reau. Solid State Ionics **107**, 293 (1998).
[38] A.I. Livshits, V.M. Buznik, P.P. Fedorov, B.P. Sobolev. Neorgan. materialy **18**, 135 (1982). (in Russian).
[39] N.I. Sorokin, M.V. Fominykh, E.A. Krivandina, Z.I. Zhmurova, B.P. Sobolev. Kristallografiya **41**, 310 (1996). (in Russian).
[40] N.I. Sorokin, B.P. Sobolev. FTT, **50**, 402 (2008). (in Russian).
[41] A. Roos, F.C.M. van de Pol, R. Keim, J. Schoonman. Solid State Ionics **13**, 191 (1984).
[42] N.A. Ivanovskaya, D.N. Karimov, N.I. Sorokin, B.P. Sobolev. Tez. dokl. VIII International Conference „Crystallophysics and deformation behavior of promising materials“ NUST MISiS, M. (2019). (in Russian). P. 103.
[43] N. Melnikova, V. Bodnar, O. Glumov, I. Murin. Tez. dokl. XII international. confer. „Fundamental problems of solid state ionics“. Izd. gruppa „Granitsa“, Chernogolovka (2014). P. 175. (in Russian).